Non-uniformity of displacement and strain within the Achilles tendon is affected by joint angle configuration and differential muscle loading

Maas, Huub; Noort, Wendy; Baan, Guus C.; Finni, Taija

Link to publication in VU Research Portal

Non-uniformity of displacement and strain within the Achilles tendon is affected by joint angle configuration and differential muscle loading

Huub Maas [a,*], Wendy Noort [a], Guus C. Baan [a], Taija Finni [b]

[a] *Department of Human Movement Sciences, Faculty of Behavioural and Movement Sciences, Vrije Universiteit Amsterdam, Amsterdam Movement Sciences, the Netherlands*
[b] *Neuromuscular Research Center, Faculty of Sport and Health Sciences, University of Jyväskylä, Finland*

ABSTRACT

Although the Achilles tendon (AT) has been studied for more than a century, a complete understanding of the mechanical and functional consequences of AT structural organization is currently lacking. The aim of this study was to assess how joint angle configuration affects subtendon displacement and strain of soleus (SOL) and lateral gastrocnemius (LG) muscles. Knots sutured onto SOL and LG subtendons of 12 Wistar rats, were videotaped to quantify displacements and the ankle torque was assessed for different isometric activation conditions (i.e., individual and simultaneous) of the triceps surae muscles. Changing ankle and knee joint angle affected the magnitude of displacement, relative displacement and strain of both SOL and LG subtendons. SOL subtendon behavior was not only affected by changes in ankle angle, but also by changes in knee angle. Displacement of SOL subtendon decreased (28–49%), but strain increased in response to knee extension. Independent of joint angle configuration, stimulation of any combination of the muscles typically resulted in displacements and strains of LG and SOL subtendons. Typically SOL displaced more but LG displaced more when stimulated at longer muscle lengths. Our results demonstrate that the distinct subtendons of the Achilles tendon can move and deform differently, but are not fully independent. Within the AT, there appears to be a precarious balance between sliding allowance and mechanical connectivity between subtendons.

© 2020 Elsevier Ltd. All rights reserved.

1. Introduction

Although the Achilles tendon (AT) has been studied for more than a century, the interest in the structure and function of its subtendons arising from the triceps surae muscles is rather recent. These subtendons are distinct to a large degree and they rotate along the proximal-distal axis (Cummins et al., 1946; Edama et al., 2015; Finni et al., 2018; Parsons, 1894; Szaro et al., 2009). However, a complete understanding of the mechanical and functional consequences of this structural organization is currently lacking. The presence of distinct subtendons of soleus (SOL), lateral (LG) and medial gastrocnemius muscles (MG) may facilitate independent transmission of muscle forces to the calcaneal bone and, hence, distinct mechanical effects of each muscle at the ankle joint (Haraldsson et al., 2008).

Non-uniform displacements within the AT, as assessed using ultrasound-based methods, have been reported during passive ankle movement (Arndt et al., 2012), during eccentric loading of

the calf muscles (Slane and Thelen, 2014) and during human walking (Franz et al., 2015). In the distal part of the AT, the anterior (deep) portion is generally associated with the SOL subtendon and the posterior (superficial) portion with the MG subtendon (Edama et al., 2015; Szaro et al., 2009). The above results suggest some degree of independence between AT subtendons, but in human studies unequivocal identification of the individual AT subtendons is not yet possible.

While non-uniform displacements within the AT indicate some degree of independence between AT subtendons, it does not exclude some connectivity. Relative sliding of the subtendons will strain the inter-subtendon matrix, which may result in force transmission between the subtendons. The matrix between fascicles within equine (Thorpe et al., 2015) and rat Achilles tendons (Maas et al., 2018) was found to be of sufficient strength to bear forces when substantial sliding (i.e. 5–8% of tendon length) occurs. Recently, it was shown that by activating SOL muscle selectively, or all triceps surae muscles together, SOL subtendon strained more than LG subtendon. On the other hand, when LG muscle was selectively stimulated, LG subtendon strained more than SOL subtendon although they underwent similar overall displacement (Finni et al., 2018). This suggests indirectly, that while force transmission via

---

the inter-subtendon matrix is possible, there is also flexibility in the system allowing movement within the tendon.

Several factors could contribute to the non-uniform deformations of AT subtendons. The stiffness of the subtendons could be different, for which there is some indirect evidence (Farris et al., 2013; Finni et al., 2018; Lichtwark et al., 2013; Obst et al., 2016). The subtendons could be loaded by different muscle forces (Arndt et al., 1999; Arndt et al., 1998; Handsfield et al., 2017), which could be caused by differential muscle activation or the muscles acting at different parts of their length-force curves. Because SOL does not span the knee joint, the length and relative position of gastrocnemius muscle can be modified independently by changes of knee joint angle. In our previous study, we investigated effects of differential muscle activation on subtendon deformations, but kept the position of the knee and ankle joints constant (Finni et al., 2018). In humans, several previous studies involving both passive and active muscle conditions reported no effects of knee joint angle on non-uniformities in the displacement within the AT (Bogaerts et al., 2018; Franz and Thelen, 2015; Stenroth et al., 2019). Effects of knee angle on strains within the various subtendons of the AT have not been studied.

Therefore, the aim of this study was to assess how joint angle configuration (affecting muscle length and relative position) affects SOL and LG subtendon behavior (i.e., displacement, relative displacement and strain). This aim was tested for different activation conditions (i.e., individual and simultaneous) of the triceps surae muscles. We hypothesized that changes in knee angle will not only affect deformations of LG subtendon, but also of SOL subtendon behavior.

2. Methods

2.1. Animals

Data were obtained from 12 adult male Wistar rats (235.5 ± 16.5 g). Surgical and experimental procedures followed the guidelines and regulations concerning animal welfare and experimentation set forth by the Dutch law and were approved by the institutional Committee on Ethics of Animal Experimentation at the Vrije Universiteit Amsterdam (#FBW12-01).

According to standard procedures in our laboratory (Maas et al., 2001), the rats were deeply anesthetized by intraperitoneal injection of urethane solution (1.2 ml/100 g body mass, 12.5% urethane solution). If withdrawal reflexes could still be elicited, supplemental doses (0.3–0.5 ml/time) were administered. Animals were placed on an electrical heating pad to keep their core temperature at approximately 37 °C. After completion of the experiments, the animals were euthanized with an overdose of pentobarbital sodium (Euthasol 20%) injected intracardially, and double-sided pneumothorax.

2.2. Surgical preparations and fixation in experimental setup

Surgical procedures were the same as those described previously (Finni et al., 2018). This study also revealed that the morphology of rat AT is very similar to that of human AT. The left hindlimb was shaved. The skin covering the lower leg and the biceps femoris were removed. The femur was exposed for later fixation of a clamp. Anatomical landmarks for axis of rotation of ankle (medial and lateral malleoli) and knee joints (origin of medial and lateral collateral ligament) were identified and marked with a permanent marker (Tijs et al., 2014). The AT was freed from all connective and fat tissues leaving the insertion to the calcaneal bone intact. For assessment of tendon deformations, four knotted suture markers (Mariderm Schwarz, 7/0, Catgut GmbH, Germany) were

sutured into each of the LG and SOL subtendons (Fig. 1). All exposed tissues were regularly irrigated with saline.

The foot was attached to a 6 degrees-of-freedom load cell (Mini40-E, ATI, Apex, NC, USA) and the femur was rigidly secured to the setup (for details see Tijs et al., 2014). The center of rotation of ankle and knee joint were aligned with the set-up's rotational axes. The set-up allowed for manipulation of ankle and knee joint angles in the sagittal plane exclusively (Fig. 1). Wire electrodes for intramuscular stimulation were inserted near the neuromuscular junctions of SOL, LG and MG muscles (for details see Tijs et al., 2014, 2016). As the threshold current near a motor endplate is substantially lower than direct excitation of muscle fibers (Mortimer and Bhadra, 2004), the chance of excitation of surrounding muscles was minimized. A video camera (HC-V720, Panasonic, UK) was placed orthogonal to the sagittal plane with focus on the AT. A ruler was placed below the tendon from which 5 mm length was digitized and used for calibration (Fig. 1B), which yielded an average resolution of 0.023 mm/pixel (range 0.022–0.024).

2.3. Experimental protocol

For each muscle, stimulation intensity was defined as the intensity resulting in the highest twitch torque. Two conditioning twitches with 1 s in between were followed by a 1 s tetanic stimulus (stimulation frequency 100 Hz, pulse width 100 μs). Two minutes rest was given between contractions. To monitor changes in muscle force producing capacity, control trials with ankle and knee joints at 90° (A90K90) with all SOL + LG + MG muscles stimulated were performed before, three times during and after the experiment. There was no effect of time on control torques (p = 0.970, repeated measures ANOVA), and the post control trial (39.5 ± 6.7 mNm) was not significantly different from the pre control (39.9 ± 8.5 mNm; p = 0.807, paired *t*-test). During each contraction, forces and moments measured by the load cell (sampled at 1000 Hz) and images of the AT (50 frames/s) were acquired.

Marker displacements and ankle joint moments were assessed for four different joint configurations and four muscle stimulation conditions of which the order was randomized between animals. The four joint angle configurations were: (i) ankle joint at 120° and knee joint at 60° (A120K60), (ii) ankle joint at 120° and knee joint at 90° (A120K90), (iii) ankle joint at 120° and knee joint at 120° (A120K120), (iv) ankle joint at 90° and knee joint at 90° (A90K90). Note that in the (i), (ii) and (ii) conditions only the knee angle is manipulated, changing the length of LG and MG but not that of SOL (Fig. 1D). The four muscle stimulation conditions were: (i) SOL only, (ii) SOL, LG and MG together, (iii) LG and MG together, (iv) LG only.

2.4. Data analysis

Three-dimensional gravity-corrected ankle torques were calculated following previously described procedures (Tijs et al., 2014). Passive torque was obtained from a 50 ms time window in relaxed condition (after the second twitch). This was subtracted from the torque obtained from a 50 ms window during the tetanic contraction to obtain the active torque used in the statistical analysis.

An image captured in the relaxed condition (after the second twitch corresponding to the passive torque) and an image during the tetanic contraction (corresponding to the time of active torque) were extracted for further analysis of tendon marker displacements. From these two images, the tendon markers were digitized manually by selecting the centroid of the knot (Finni et al., 2018), and [x, y] coordinates were extracted. Image analysis was done using custom written software in MATLAB (R2014b, Mathworks, Natick, MA, USA).
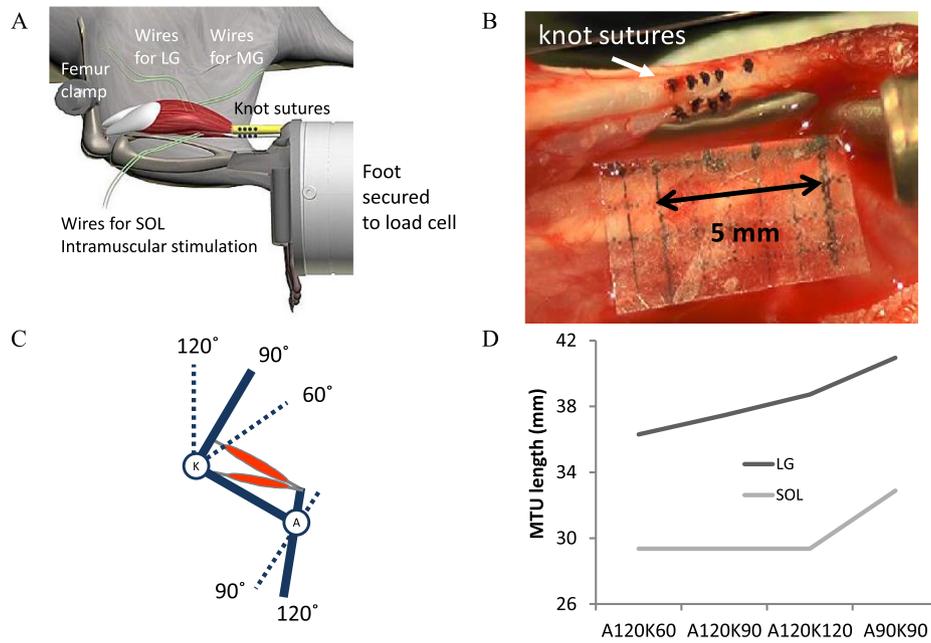
Fig. 1. Schematics of experimental setup and joint configurations. (A) Lateral view of the rat left hindlimb in the set-up. The femur was fixed and the foot was attached to the load cell. Wire electrodes within soleus (SOL), medial (MG) and lateral gastrocnemius (LG) muscle bellies were used for intramuscular stimulation. Knot sutures in LG (top row) and SOL subtendons (bottom row) are shown as black dots. (B) Picture of Achilles tendon in experimental setup showing the knot sutures in the LG (top row of knots) and SOL subtendons (bottom row of knots). (C) A schematic of the rat hind limb, indicating the different imposed angles of the ankle (A, 90° and 120°) and knee joints (K, 60°, 90° and 120°). (D) Estimated muscle-tendon unit (MTU) lengths of LG and SOL muscles for the four joint configurations (i.e., combinations of ankle and knee angles) tested. As SOL muscle does not cross the knee joint, the MTU length of only LG will be altered in three of the four joint configurations.

From the [x, y] coordinates, displacement (D) of each of the markers (*n*) from passive to active state (Δx and Δy) was calculated. Then the average displacement ($\bar{D}$) was calculated as the mean of the four SOL and four LG marker displacements, respectively.

$$D_n = \sqrt{\Delta x_n^2 + \Delta y_n^2} \quad n = 1, 2, 3, 4$$

$$D = \frac{D_1 + D_2 + D_3 + D_4}{4}$$

Relative displacement (ΔD) was calculated as:

$$D = D_{LG} - D_{SOL}$$

Strains (ε) based on a linear 3-segment model connecting the four markers in SOL and LG subtendons, respectively, were calculated as $\varepsilon = (L - L_0)/L_0$, where L was the 3-segment length in an active state and L_0 the 3-segment length in the passive state.

Average LG and SOL muscle-tendon unit lengths were estimated (Fig. 1D) using an ankle-knee geometric model (Bernabei et al., 2017). The following anatomical parameters, required in the model, were measured from the animals of the present study: ankle lever arm length (6.8 mm, SD 0.69) and tibia length (38.3 mm, SD 1.01).

2.5. Statistics

Normal distribution of the data was checked with the Shapiro-Wilk test, by comparing mean and median values, and by checking values of skewness and kurtosis. There was no strong evidence for non-normal distribution and parametric statistics were used. A two-way repeated measures ANOVA (joint configuration × stimulation) was used to examine differences in torque and relative displacement between conditions (Huyhn-Feldt correction was used in case of violation of sphericity). The effects of joint configuration on average displacement and within subtendon strains of SOL and LG subtendons was examined separately at each stimulation condition with two-way repeated measures ANOVAs (joint configuration × subtendon). In case of significant interaction, Bonferroni corrected t-tests were performed (i.e. p-values were multiplied by the number of comparisons). Effect sizes from ANOVA (Partial Eta Squared, $\eta^2_{partial}$) are reported. Level of significance was set at $p \leq 0.05$.

3. Results

3.1. Ankle joint torque

There were main effects of joint configuration (p = 0.034, $\eta^2_{partial}$ = 0.279) and stimulation (p < 0.001, $\eta^2_{partial}$ = 0.965) on ankle
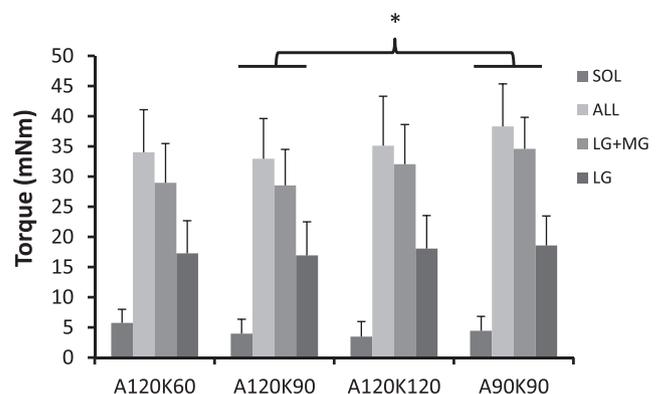
Fig. 2. Effects of joint configuration (x-axis) and muscle stimulation condition (different colour bars) on ankle plantarflexion torque. Each stimulation condition differed significantly in each joint configuration. Overall differences in torque between joint angles (A, ankle; K, knee) were found between A120K90 and A90K90 (p = 0.004). SOL, soleus; LG, lateral gastrocnemius; MG, medial gastrocnemius. ** indicates p < 0.01. Means + SD are shown (n = 12).

torque, and a significant interaction ($p = 0.001$, $\eta^2_{partial} = 0.359$) (Fig. 2). Pairwise comparisons revealed overall effects of joint configuration on torque only between A120K90 and A90K90 ($p = 0.004$), torques being higher in the latter condition. All stimulation conditions produced significantly different torques at each angle (all $p < 0.001$).

3.2. Subtendon displacement

When SOL was stimulated, displacements of SOL and LG subtendons were different ($p = 0.001$, $\eta^2_{partial} = 0.650$). There was also a main effect of joint configuration ($p < 0.001$, $\eta^2_{partial} = 0.663$), but no significant interaction ($p = 0.083$, $\eta^2_{partial} = 0.198$) (Fig. 3A). Pairwise comparisons revealed that SOL displacement was greater than LG displacement (ranging from 23% to 93%) at each joint configuration tested ($p \leq 0.010$).

When SOL + LG + MG were stimulated, displacements of SOL and LG subtendons were different ($p = 0.003$, $\eta^2_{partial} = 0.571$), there was a main effect of joint configuration ($p < 0.001$, $\eta^2_{partial} = 0.658$) and a significant interaction ($p = 0.002$, $\eta^2_{partial} = 0.364$) (Fig. 3B). Pairwise comparisons revealed that SOL displacement was greater than LG at joint configurations A120K60 (7%, $p = 0.004$), A120K90 (6%, $p = 0.002$) and A120K120 (6%, $p = 0.013$).

When LG + MG were stimulated, displacements of SOL and LG subtendons were different ($p = 0.030$, $\eta^2_{partial} = 0.362$), there was a main effect of joint configuration ($p < 0.001$, $\eta2_{partial} = 0.712$), and a significant interaction ($p < 0.001$, $\eta^2_{partial} = 0.537$) (Fig. 3C). Pairwise comparisons indicated that LG displacement was greater than SOL at A120K120 (7%, $p = 0.009$) and A90K90 (20%, $p = 0.001$).

When LG was stimulated, SOL and LG subtendon displacements were similar ($p = 0.747$, $\eta^2_{partial}$ 0.010), but there was a main effect of joint configuration ($p < 0.001$, $\eta^2_{partial} = 0.662$), and a significant interaction ($p < 0.001$, $\eta^2_{partial} = 0.499$) (Fig. 3D). Pairwise comparisons indicated that SOL displaced 6% more than LG at A120K60 ($p = 0.044$), but at A90K90 LG displacement was 21% greater than SOL ($p = 0.022$).

These results indicate that joint angle configuration affects subtendon displacement both when muscles are stimulated and when some of the muscles were passive. Displacement of SOL subtendon was significantly affected by changes in knee angle (all $p \leq 0.011$).

3.3. Relative displacement between subtendons

Main effects of joint configuration ($p < 0.001$, $\eta^2_{partial} = 0.503$) and stimulation ($p = 0.002$, $\eta^2_{partial} = 0.552$) on relative subtendon displacement were found, without significant interaction ($p = 0.068$, $\eta^2_{partial} = 0.162$). Pairwise comparisons revealed overall differences in relative displacement at joint configurations of A120K60 vs. A90K90 ($p = 0.009$) and A120K90 vs. A90K90 ($p = 0.012$), relative displacements being higher (i.e. LG moved more than SOL subtendon) in the A90K90 condition (Fig. 4). These results indicate that relative displacement between SOL and LG subtendons is affected independently by joint configuration as well as stimulation condition.

3.4. Subtendon strain

When SOL was stimulated, strains of SOL and LG subtendons were different ($p < 0.001$, $\eta^2_{partial} = 0.879$), there was a main effect of joint configuration ($p = 0.001$, $\eta^2_{partial} = 0.402$) and a significant interaction ($p < 0.001$, $\eta^2_{partial} = 0.583$) (Fig. 5A). Pairwise comparisons indicated that at each joint configuration SOL strain was several times (77–479%) greater than LG strain ($p \leq 0.025$).

When SOL + LG + MG was stimulated, strains of SOL and LG subtendons were different ($p = 0.003$, $\eta^2_{partial} = 0.563$), there was a main effect of joint configuration ($p < 0.001$, $\eta^2_{partial} = 0.473$) and a significant interaction ($p < 0.001$, $\eta^2_{partial} = 0.633$) (Fig. 5B). Pairwise comparisons revealed that strain in SOL subtendon was greater than in LG at A120K90 (79%, $p = 0.001$), A120K120 (116%, $p < 0.001$) and A90K90 (68%, $p = 0.011$).

When LG + MG was stimulated, strains of SOL and LG subtendons were different ($p < 0.001$, $\eta^2_{partial} = 0.856$), there was a main
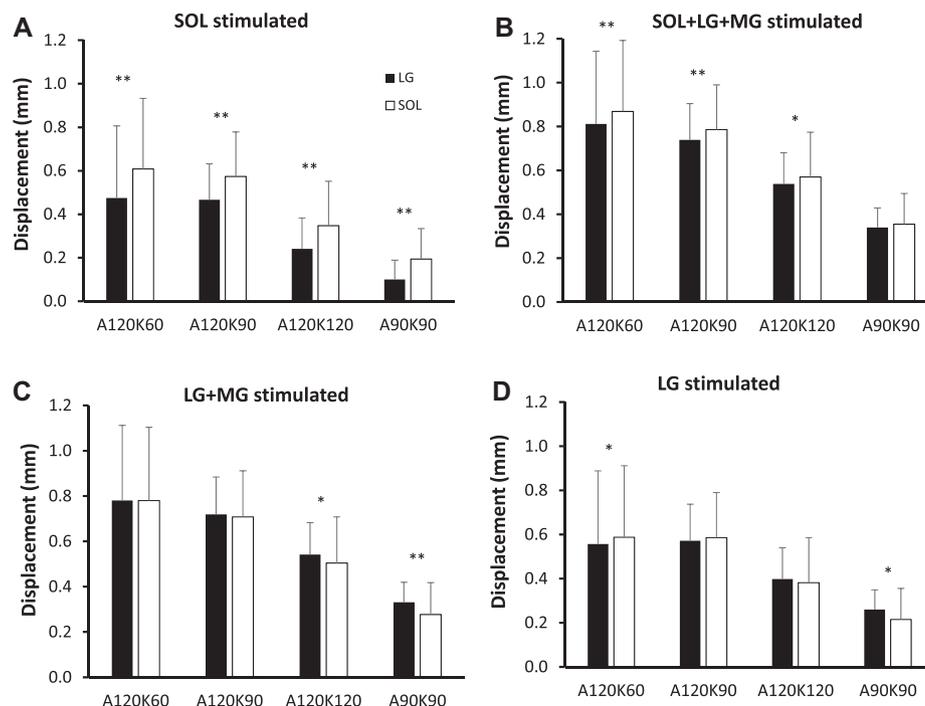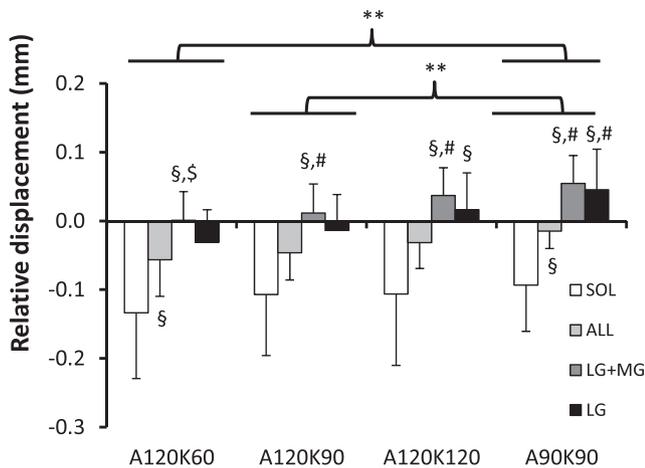

Fig. 3. Effects of joint configuration and muscle stimulation condition on displacement of the subtendons of soleus (SOL) and lateral gastrocnemius (LG) muscles. Means + SD are shown (n = 12). MG, medial gastrocnemius muscle. Significant differences between SOL and LG subtendons: * $p < 0.05$; ** $p < 0.01$.

Fig. 4. Relative displacement of soleus (SOL) and lateral gastrocnemius (LG) subtendons for different joint configurations and stimulation conditions. Negative values mean that SOL subtendon moved more than LG subtendon (see Methods). Means +/- SD are shown (n = 12). Significant differences between joint configurations: ** p < 0.01. At a given joint angle configuration, § indicates that the relative displacement for that stimulation condition was significantly different (p < 0.05) from that during SOL stimulation condition; # indicates a difference with stimulation of ALL muscles and $ indicates a difference with LG stimulation condition.

effect of joint configuration (p = 0.031, $\eta^2_{partial}$ = 0.234) and a significant interaction (p < 0.001, $\eta^2_{partial}$ = 0.677) (Fig. 5C). Pairwise comparisons showed that strain in LG was several times greater than in SOL at each joint configuration (p ≤ 0.01).

When LG was stimulated, strains of SOL and LG subtendons were different (p < 0.001, $\eta^2_{partial}$ = 0.925), there was a main effect of angle (p = 0.014, $\eta^2_{partial}$ = 0.271) and a significant interaction (p < 0.001, $\eta^2_{partial}$ = 0.666) (Fig. 5D). Pairwise comparisons indicated that the strain in LG was several times greater than in SOL at each joint configuration (p < 0.001).

Maximum strains were observed at the shortest muscle–tendon unit lengths tested for LG. For LG, maximum strain (6.3 ± 1.8%) was observed during LG stimulation at A120K60. Maximum SOL strain (8.5 ± 2.2%) was found during SOL stimulation at A120K120 (Fig. 5A). As found for displacement, SOL subtendon strain was affected by changes in knee joint angle (all stimulation conditions p < 0.015).

4. Discussion

The main finding of this study was consistent with the hypothesis showing that joint angle configuration affected the magnitude of displacement, relative displacement and strain of both SOL and LG subtendons. More specifically, SOL subtendon behavior was not only affected by changes in ankle angle, but also by changes in knee angle. Independent of joint angle configuration, stimulation of any combination of the muscles typically resulted in displacements and strains of both subtendons. Most often the SOL subtendon displaced more, but LG subtendon displaced more when LG was stimulated at longer muscle lengths (Fig. 3). Strain in the SOL or LG subtendon was greater when their representative muscle was stimulated. When all muscles were stimulated, typically SOL subtendon strained more than LG. As reported previously for the rat (Finni et al., 2018) and human AT (e.g. Arndt et al., 2012; Beyer et al., 2018; Franz et al., 2015; Slane and Thelen, 2014), we found SOL and LG subtendons to displace and strain differently in most conditions tested. Both SOL and LG subtendon displacements decreased when knee was extended and reached smallest displacement to each stimulation condition at the longest

muscle-tendon unit lengths (Fig. 3), which is in agreement with the stress-strain properties of tendon (Cui et al., 2009). We also found that the relative displacement between SOL and LG subtendons was affected independently by knee angle/joint configuration (Fig. 4). This is in contrast with several studies in human subjects in which no significant effects of knee angle on non-uniform displacements within the human AT were reported (Bogaerts et al., 2018; Franz and Thelen, 2015; Stenroth et al., 2019). This may be explained by differences in the location along the AT for which local deformations were assessed, being more proximal in our study compared to most studies in humans. It has been suggested that the subtendons are more tightly linked distally than proximally (Arndt et al., 1999).

A recent human study showed that SOL subtendon displaced more than LG at the different ankle joint angles tested and this corresponded to greater shortening of SOL than LG muscle (Clark and Franz, 2018). Indeed, it is to be expected that if a muscle is selectively stimulated, its representative tendon would move more than others. In the present study, when LG was stimulated at the longest length (A90K90), LG subtendon displacement was greater than SOL (Fig. 4). However, when LG was stimulated at the shortest length (A120K60), SOL displaced more than LG. This suggests that the sign of relative subtendon displacement is not only dependent on the level of muscle contraction. This is in contrast to strain, which was always greater when their representative muscle was stimulated; maximal strain being higher in SOL (up to ~8%) than in LG subtendon (up to ~6%). Humans studies have reported strains ranging from 3.8 to 6.6% in SOL to 2.6–2.7% in MG (see Discussion in Finni et al., 2018). However, the strain responses to changes in joint configuration differed between subtendons. Greatest strains in SOL were found at A120K90 and A120K120, while greatest LG strains were found at A120K60 (Fig. 5).

Consistent with our hypothesis, changes in knee angle did not only affect deformations of LG subtendon, but also of SOL subtendon. The differential behaviour between subtendons when joint configuration was altered, likely relates to force transmission within and between the involved tissues which can be modified by a number of factors.

Firstly, force can be transmitted between gastrocnemius and SOL muscle bellies (Bernabei et al., 2015) and/or subtendons (Maas et al., 2018). Knee movements will change the position of gastrocnemius relative to SOL and, thereby, strain connective tissues between the muscle bellies (Bojsen-Moller et al., 2010; Maas, 2009; Maas and Finni, 2018). A recent human study showed that selective activation of LG muscle can stiffen the connective tissues between SOL and LG muscle bellies, thereby, facilitating force transmission at least at short muscle lengths (Finni et al., 2018). Thus, both the relative muscle positions and activation may change the extent of intermuscular force transmission and, hence, force levels exerted at each of the subtendons.

Secondly, knee movements will affect the length of gastrocnemius subtendon and, thereby, the relative position with SOL subtendon. This will cause shear within the inter-subtendon matrix, which may facilitate inter-subtendon force transmission. Such force transmission is supported also by other observations; both subtendons moved when only one muscle was stimulated. Thus, force exerted by the stimulated muscle did not only pull on the corresponding subtendon but also on the other one.

Displacements do not provide information about the magnitude of the forces involved, but SOL stimulation resulted also in substantial strains in LG subtendon. In addition, SOL subtendon strain was found in response to LG stimulation, but to a smaller degree. As strain is a function of stress, these results indicate that part of the force produced by the muscle fibers in one muscle is transmitted via the inter-subtendon matrix to the subtendon of the neighboring muscle.
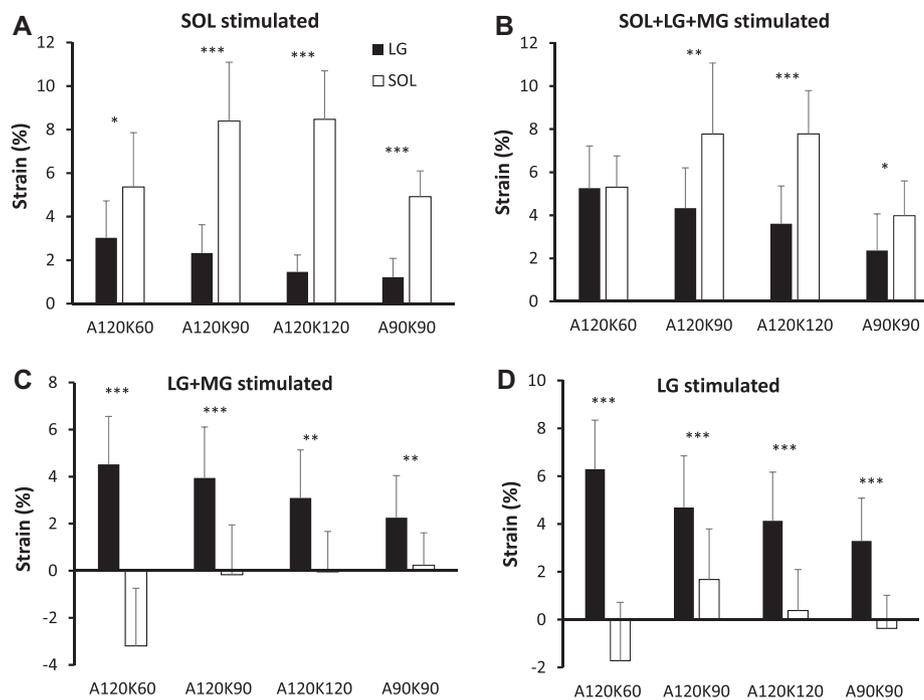
Fig. 5. Effects of joint configuration and muscle stimulation condition on strain of soleus (SOL) and lateral gastrocnemius (LG) subtendons. Means + SD are shown (n = 12). Significant differences between SOL and LG subtendon strain: * $p < 0.05$, ** $p < 0.01$, *** $p < 0.001$.

Differences in strain between SOL and LG subtendons were substantially higher than differences in displacement. When both LG and MG were stimulated simultaneously, strain was observed in LG subtendon exclusively in three of the joint configurations, indicating that the proximal portion of SOL subtendon was not deformed. Although it is clear that the SOL and LG subtendons exert some force on each other resulting in similar displacements, the strains suggest that most force produced by each muscle is transmitted via its own subtendon.

It should be noted that displacements and strains were assessed for only part of the AT, the most proximal portion of SOL subtendon and the mid-portion of LG subtendon. The mechanical effects of relative displacements proximally may be more pronounced distally. In addition, marker displacements were measured in two-dimensions. Out-of-plane movements, for example due to possible rotation of the tendon, were not captured (see also Finni et al., 2018). This may explain the observed negative strains in SOL subtendon in response to stimulation of LG and LG+MG muscles (Fig. 5).

Sliding within AT may be necessary to allow muscles crossing one (SOL) or two joints (gastrocnemius) with independent activation patterns (Moritani et al., 1991) to function normally, and lack of sliding may be a sign of malfunction. In a surgically repaired tendon, relative displacements were reported to be completely absent even one year post-surgery (Beyer et al., 2018), which may be due to scar tissue. On the other hand, because the inter-subtendon matrix can bear considerable loads (Maas et al., 2018), forces produced by the triceps surae can be distributed within the whole AT. We proposed recently that the inter-subtendon matrix provides an alternative pathway for force transmission and may serve to minimize peak stresses and, thereby, may prevent tendon injuries (Maas and Finni, 2018). The above suggests a precarious balance between sliding allowance and mechanical connectivity between fascicles and subtendons within the AT.

As a conclusion, our results demonstrate that the distinct subtendons of the Achilles tendon can move and deform differently, but are not fully independent. SOL subtendon displacement and strain were affected by knee joint angle that was likely due to force transmission via the intermuscular and intersubtendon matrices. Subtendon strain was affected by changes in joint configuration and muscle stimulation differently than subtendon displacement.

Declaration of Competing Interest

The authors declare that they have no known competing financial interests or personal relationships that could have appeared to influence the work reported in this paper.

References

Arndt, A., Bengtsson, A.S., Peolsson, M., Thorstensson, A., Movin, T., 2012. Non-uniform displacement within the Achilles tendon during passive ankle joint motion. Knee Surg. Sports Traumatol. Arthrosc. 20, 1868–1874.

Arndt, A., Bruggemann, G.P., Koebke, J., Segesser, B., 1999. Asymmetrical loading of the human triceps surae: I. Mediolateral force differences in the Achilles tendon. Foot Ankle Int. 20, 444–449.

Arndt, A.N., Komi, P.V., Bruggemann, G.P., Lukkariniemi, J., 1998. Individual muscle contributions to the in vivo achilles tendon force. Clin. Biomech. (Bristol, Avon) 13, 532–541.

Bernabei, M., Dieën, J.H.v., Maas, H., 2017. Longitudinal and transversal displacements between triceps surae muscles during locomotion of the rat. J. Exp. Biol. 220, 537–550.

Bernabei, M., van Dieen, J.H., Baan, G.C., Maas, H., 2015. Significant mechanical interactions at physiological lengths and relative positions of rat plantar flexors. J. Appl. Physiol. 118, 427–436.

Beyer, R., Agergaard, A.S., Magnusson, S.P., Svensson, R., 2018. Speckle tracking in healthy and surgically repaired human Achilles tendons at different knee angles—a validation using implanted tantalum beads. Translational Sports Med. 1, 79–88.

Bogaerts, S., De Brito Carvalho, C., De Groef, A., Suetens, P., Peers, K., 2018. Non-uniformity in pre-insertional Achilles tendon is not influenced by changing knee angle during isometric contractions. Scand. J. Med. Sci. Sports 28, 2322–2329.

Bojsen-Moller, J., Schwartz, S., Kalliokoski, K.K., Finni, T., Magnusson, S.P., 2010. Intermuscular force transmission between human plantarflexor muscles in vivo. J. Appl. Physiol. 109, 1608–1618.

Clark, W.H., Franz, J.R., 2018. Do triceps surae muscle dynamics govern non-uniform Achilles tendon deformations?. PeerJ 6, e5182.

Cui, L., Maas, H., Perreault, E.J., Sandercock, T.G., 2009. In situ estimation of tendon material properties: differences between muscles of the feline hindlimb. J. Biomech. 42, 679–685.

Cummins, E.J., Anson, B.J., Carr, B.W., Wright, R.R., Hauser, E.D.W., 1946. The structure of the calcaneal tendon (of Achilles) in relation to orthopedic surgery - with additional observations on the plantaris muscle. Surg. Gynecol. Obstet. 83, 107–116.

Edama, M., Kubo, M., Onishi, H., Takabayashi, T., Inai, T., Yokoyama, E., Hiroshi, W., Satoshi, N., Kageyama, I., 2015. The twisted structure of the human Achilles tendon. Scand. J. Med. Sci. Sports 25, e497–e503.

Farris, D.J., Trewartha, G., McGuigan, M.P., Lichtwark, G.A., 2013. Differential strain patterns of the human Achilles tendon determined in vivo with freehand three-dimensional ultrasound imaging. J. Exp. Biol. 216, 594–600.

Finni, T., Bernabei, M., Baan, G.C., Noort, W., Tijs, C., Maas, H., 2018. Non-uniform displacement and strain between the soleus and gastrocnemius subtendons of rat Achilles tendon. Scand. J. Med. Sci. Sports 28, 1009–1017.

Franz, J.R., Slane, L.C., Rasske, K., Thelen, D.G., 2015. Non-uniform in vivo deformations of the human Achilles tendon during walking. Gait Posture 41, 192–197.

Franz, J.R., Thelen, D.G., 2015. Depth-dependent variations in Achilles tendon deformations with age are associated with reduced plantarflexor performance during walking. J. Appl. Physiol. 1985 (119), 242–249.

Handsfield, G.G., Inouye, J.M., Slane, L.C., Thelen, D.G., Miller, G.W., Blemker, S.S., 2017. A 3D model of the Achilles tendon to determine the mechanisms underlying nonuniform tendon displacements. J. Biomech. 51, 17–25.

Haraldsson, B.T., Aagaard, P., Qvortrup, K., Bojsen-Moller, J., Krogsgaard, M., Koskinen, S., Kjaer, M., Magnusson, S.P., 2008. Lateral force transmission between human tendon fascicles. Matrix Biol. 27, 86–95.

Lichtwark, G.A., Cresswell, A.G., Newsham-West, R.J., 2013. Effects of running on human Achilles tendon length-tension properties in the free and gastrocnemius components. J. Exp. Biol. 216, 4388–4394.

Maas, H., 2009. Mechanical interactions between skeletal muscles. In: Shinohara, M. (Ed.), Advances in Neuromuscular Physiology of Motor Skills and Muscle Fatigue. Research Signpost, Kerala, India, pp. 285–302.

Maas, H., Baan, G.C., Huijing, P.A., 2001. Intermuscular interaction via myofascial force transmission: effects of tibialis anterior and extensor hallucis longus length on force transmission from rat extensor digitorum longus muscle. J. Biomech. 34, 927–940.

Maas, H., Cesa Correira, J., Baan, G.C., Noort, W., Screen, H.R., 2018. Force transmission between Achilles subtendons of rat. World Congress of Biomechanics, Dublin, Ireland.

Maas, H., Finni, T., 2018. Mechanical coupling between muscle-tendon units reduces peak stresses. Exerc. Sport Sci. Rev. 46, 26–33.

Moritani, T., Oddsson, L., Thorstensson, A., 1991. Phase-dependent preferential activation of the soleus and gastrocnemius muscles during hopping in humans. J. Electromyogr. Kinesiol. 1, 34–40.

Mortimer, J.T., Bhadra, N., 2004. Peripheral nerve and muscle stimulation. In: Horch, K.W., Dhillon, G.S. (Eds.), Neuroprosthetics: Theory and Practice, 2. World Scientific Publishing Company, River Edge, NJ, pp. 638–682.

Obst, S.J., Newsham-West, R., Barrett, R.S., 2016. Changes in Achilles tendon mechanical properties following eccentric heel drop exercise are specific to the free tendon. Scand. J. Med. Sci. Sports 26, 421–431.

Parsons, F.G., 1894. On the morphology of the Tendo-Achillis. J Anat Physiol 28, 414–418.

Slane, L.C., Thelen, D.G., 2014. Non-uniform displacements within the Achilles tendon observed during passive and eccentric loading. J. Biomech. 47, 2831–2835.

Stenroth, L., Thelen, D., Franz, J., 2019. Biplanar ultrasound investigation of in vivo Achilles tendon displacement non-uniformity. Transl Sports Med 2, 73–81.

Szaro, P., Witkowski, G., Smigielski, R., Krajewski, P., Ciszek, B., 2009. Fascicles of the adult human Achilles tendon - an anatomical study. Ann. Anat. 191, 586–593.

Thorpe, C.T., Godinho, M.S., Riley, G.P., Birch, H.L., Clegg, P.D., Screen, H.R., 2015. The interfascicular matrix enables fascicle sliding and recovery in tendon, and behaves more elastically in energy storing tendons. J. Mech. Behav. Biomed. Mater. 52, 85–94.

Tijs, C., van Dieen, J.H., Baan, G.C., Maas, H., 2014. Three-dimensional ankle moments and nonlinear summation of rat triceps surae muscles. PLoS ONE 9, e111595.

Tijs, C., van Dieen, J.H., Baan, G.C., Maas, H., 2016. Synergistic co-activation increases the extent of mechanical interaction between rat ankle plantar-flexors. Front. Physiol. 7, 414.